Biometals (2024) 37:1289–1303
https://doi.org/10.1007/s10534-024-00610-4

RESEARCH

Iron oxide nanoparticles derived from *Polyalthia korintii* (Dunal) Benth. & Hook. F leaves extract exhibits biological and dye degradation potentials

K. E. Hana Mol · Tancia Rosalin · K. K. Elyas

Received: 12 October 2023 / Accepted: 10 May 2024 / Published online: 5 September 2024

Abstract Green synthesis of iron oxide nanoparticles using plant extracts is of tremendous interest owing to its cost effectiveness, ecofriendly and high efficiency compared to physical and chemical approaches. In the current study, we describe a green approach for producing iron oxide nanoparticles utilizing *Polyalthia korintii* aqueous leaf extract (PINPs). The prepared PINPs were assessed of their biological and dye degradation potentials. The physico-chemical characterization of PINPs using UV–Visible spectrophotometer, Fourier Transform Infrared Spectroscopy, X-Ray Diffraction studies, Field emission Scanning Electron Microscopy and Energy Dispersive X-ray spectroscopy analysis confirmed the synthesized sample comprised of iron oxide entity, predominantly spherical with the size range of 40–60 nm. Total Phenolic Content of PINPs is 59.36±1.64 µg GAE/mg. The PINPs exhibited 89.78±0.07% DPPH free radical scavenging and 28.7±0.21% ABTS cation scavenging activities. The antibacterial activities were tested against different gram-positive and gram-negative bacteria and PINPs were more effective against *Enterococcus faecalis* and *Klebsiella pneumoniae*. Cytotoxicity of PINPs against K562 and HCT116 were measured and IC50 values were found to be 84.99±4.3 µg/ml and 79.70±6.2 µg/ml for 48 h respectively. The selective toxicity of PINPs was demonstrated by their lowest activity on lymphocytes, HEK293 cells, and erythrocytes. The toxicity (LC 50 values) against first, second, third and fourth instar larvae of *Culex quinquefasciatus* was 40±1.5 mg/mL, 45±0.8 mg/mL, 99±2.1 mg/mL and 120±3.5 mg/mL respectively. Finally, PINPs were utilized to as a catalyst for removal of textile dyes like Methylene blue and methyl orange in a fenton-like reaction. The results showed 100% dye degradation efficiency in a fenton like reaction within 35 min. Thus, the green synthesized PINPs exhibit antioxidant, antibacterial, antiproliferative, larvicidal and dye degradation potentials, indicating their suitability for biological and environmental applications.

Keywords Iron Nanoparticles · PINPs · Polyalthia korintii · Antioxidant activity · Antiproliferative activity · Dye degradation activity · Methylene Blue · Methyl Orange

Abbreviations

INP	Iron Nanoparticles;
PINPs	*Polyalthia korintii* Iron oxide nanoparticles;

K. E. H. Mol · T. Rosalin (✉) · K. K. Elyas
Immunotechnology Lab, Department of Biotechnology, University of Calicut, Malappuram 673635, Kerala, India
e-mail: tanciarosalin@gmail.com

K. E. H. Mol
e-mail: hana.basheerke@gmail.com

K. K. Elyas
e-mail: kkelyas@yahoo.com

T. Rosalin
Department of Integrated Biology, St. Joseph's College (Autonomous), Irinjalakuda, Thrissur 680121, Kerala, India

FTIR	Fourier-transform infrared spectroscopy;
XRD	X-ray diffractometer;
FESEM	Field emission scanning electron microscopy;
EDX	Energy dispersive X-ray;
DPPH	2,2-Diphenylpicrylhydrazyl;
ABTS	2,2′-Azino-bis(3-ethylbenzothiazoline-6-sulfonic acid);
MIC	Minimum Inhibitory Concentration;
MBC	Minimum Bactericidal Concentration;
GAE/mg	Gallic Acid Equivalent

Introduction

Traditional methods of nanoparticle synthesis often involve high energy consumption and inclusion of harmful chemicals. In contrast, green synthesis offers an environmental friendly and cost-effective method using bio-friendly natural resources, thus avoiding negative impacts on the environment and human health (Tahir et al. 2016; Cai et al. 2014; Poguberović et al. 2016). Researchers are concentrating more on promoting green synthesis as they have the additional advantage of performance under mild reaction conditions, affordability and easy scalability. Usage of biocompatible materials also provides the nanoparticles with special features that make them appropriate for a variety of applications, including environmental cleanup, drug delivery, biosensors, and catalysis. Furthermore, encouraging the utilization of renewable resources can contribute to the reduction of waste generation and carbon emissions.

Iron nanoparticles (INPs) have been a subject of intensive research in recent years because of their wide range of applications. Various forms of INPs have been observed, including zero valent iron nanoparticles, iron oxide nanoparticles, and iron oxide hydroxide nanoparticles (Poguberović et al. 2016; Hassan and Hameed 2011). They have been used in a variety of applications including drug delivery, magnetic targeting, hyperthermia, gene therapy, negative MRI contrast enhancement, food preservation, antimicrobial agents, bio-separation, environmental remediation, and lithium-ion batteries because of their special physicochemical properties, high catalytic activity, high magnetism, low toxicity, and microwave absorption capacity (Chan et al. 2022; Ali et al. 2021; Anik et al. 2021; Yalcin and Gündüz 2021; Avasthi et al. 2020). Iron oxide nanoparticles are the most extensively used for bioremediation due to their magnetic properties and recyclability. They are also advantageous for biological applications owing to their minimal toxicity and reduced adverse effects (Avasthi et al. 2020).

Polyalthia korintii is an Indo—Sri Lankan ethnomedicinal species bearing edible fruits (Ashton et al. 1997) and is mainly confined to the biodiversity hotspots of India—the Eastern Ghats and the southern Western Ghats (Richard and Muthukumar 2012). The presence of this species is mainly reported from sacred grooves and reserve forests in India. For instance, it is reported from Sree puthiya bhagavathi sacred grove, Kalloori in Kannur district, Kerala (Poovathur and Joseph 2016), Iriveri Sree Pulideva Temple associated sacred groove, Kannur district, Kerala (Swathi and Joseph 2017), Mundanthurai Range in the Kalakad-Mundanthurai Tiger Reserve (Richard and Muthukumar 2012), Cheruvathur Grama Panchayath of Kasargod district, Kerala (Sharma et al. 2003), Kadapa district of Andhra Pradesh (Sekhar et al. 2011), and Kambakam hills, Andhra Pradesh (Basha et al. 2014).

Due to its extreme localization and limited availability, the ethnomedicinal claims of *P. korintii* have been linked to tribes. The Kambakam Hill Tribes of India's Eastern Ghats employ the root bark to treat stomach aches. The village people of Kadapa (India) use root powder decoction orally as a potent remedy for Russell viper bites (Bijauliya et al. 2017). The herb is not scientifically investigated despite having medicinal qualities but is shown to contain several secondary metabolites, particularly higher amounts of alcohol soluble like phenols and flavonoids (Rosalin and Elyas 2018). The polyphenolic compounds are active metal ion chelators, reductors and capping agents which could aid in nanoparticle formation (Makarov et al. 2014; Rosa Salles et al. 2022).

The significance of this study is rooted in the fact that although other members of *Polyalthia* species have been documented as effective in synthesizing nanoparticles, there is an absence of prior research on the utilization of *P. korintii*. Additionally, the potentials of this plant remain unexplored. Therefore, this study aims to fill this research gap by investigating the nanoparticle synthesis capabilities and exploring its untapped potentials there by contributing to the advancement of our understanding of nanoparticle synthesis within *Polyalthia* species and revealing

novel opportunities for its application across diverse fields. For instance, iron oxide nanoparticles are extensively studied for water remediation, where they are used to remove dye and drug contaminants from water when traditional wastewater treatment methods are not effective (Nunes et al. 2023).

Materials and methods

Preparation of plant extract

Healthy leaves of *Polyalthia korintii* were collected from Calicut University Botanical Garden (CUBG), Kerala (11^0 8′ 5.1432″ N; 75° 53′ 26.1096'' E); and a voucher specimen (Accession No: 6917) was deposited at the University herbarium. Collected leaves were washed thrice with running tap water and then with distilled water. Then, the leaves were dried by placing them on a blotting paper for 2 h at room temperature. From this, 10 g was weighed, cut into fine pieces and boiled in 100 ml of deionized water for 20 min. The resulting extract was allowed to cool and then filtered using Whatman filter paper. The collected leaf extract was used as a reducing agent for nanoparticle synthesis and were stored at 4^0C (Silva et al. 2011).

Synthesis of PINPs

PINPs were prepared by adding 0.01 M $FeCl_3$ to the leaves extract at the volume ratio 2:3 by stirring continuously at 60^0C. After 24 h, the mixture was centrifuged at 5000 rpm for 10 min in a cooling centrifuge at 5^0C. Then the pellet was washed using deionized water and then dried in oven at 50^0C for 24–48 h (Beheshtkhoo et al. 2018; Turakhia et al. 2018).

Characterization

The green synthesized PINPs were initially characterized by change in colour after incubation and the formation of a pellet after centrifugation. Further analysis was done using a spectrophotometer using a small aliquot of sample diluted with distilled water. Later, synthesized PINPs were centrifuged and the resultant pellet was oven dried. The dried powder was taken for further analysis. The FTIR spectra were recorded at a wavelength ranging from 4000 – 400 cm^{-1}. To understand the components and phytochemicals present in the powder, the oven dried powder was pelletized with potassium bromide (KBr) and was subjected to FTIR analysis (Vivek et al. 2012). X-ray diffraction was also performed to determine the crystal structure of nanoparticles (Bhakya et al. 2016). For XRD analysis, the nanoparticles were coated on a glass substrate and XRD measurements were carried out using an X-ray diffractometer with Cu Kα radiation (40 kV, 15 mA) in 2θ configuration ranging from $20–70^0$. For morphological characterization, purified PINPs were subjected to FESEM and EDX analysis using a Carl-Zeiss Gemini 300 SEM instrument.

Phytochemical analysis

Phytochemical screening was carried out according to standard procedure (Devatha et al. 2016; Rashmi et al. 2021).

Estimation of Total Phenolic Content (TPC)

The total phenolic content of PINPs and their plant extract were determined by Folin–ciocalteau method using gallic acid as standard (Gupta and Prakash 2009) and expressed as Gallic Acid Equivalence (GAE). The reaction sample was made using ethanol (1 mg/ml) and was diluted with 4.5 ml distilled water and slowly added 0.1 ml of folin–ciocalteau reagent and was shaken for 3 min. 0.3 ml of 2% Na_2CO_3 was added. The mixture was allowed to stand for 3 h and the absorbance was read at 760 nm against blank.

In vitro Antioxidant studies:

DPPH free radical scavenging assay

Different concentrations of sample, ranging from 10–100 µg/ml were prepared in methanol. From this, 100 µl was transferred to a 96 well plate and added 100 µl DPPH (0.2 mM dissolved in methanol). The solution was mixed well and left to stand for 15 min in the dark at room temperature before the absorbance was recorded at 517 nm. Triplicates were done for all the concentrations tested. Ascorbic acid (1 mg/ml) was taken as standard, the scavenging effect was calculated using the formula:

$$\text{Scavenging rate (\%)} = \frac{(\text{Absorbance of sample} - \text{Absorbance of control})}{\text{Absorbance of control}} * 100$$

ABTS radical scavenging assay

To 96 well plate, 50 µl samples at different concentrations and 100 µl ABTS working reagent was transferred. The mixture was mixed well and left to stand for 10 min in the dark at room temperature. Then the absorbance was read at 734 nm against blank. Ascorbic acid (1 mg/ml) was taken as standard, the scavenging effect was calculated using the formula:

$$\text{Scavenging rate} = \frac{(\text{Absorbance of sample} - \text{Absorbance of control})}{\text{absorbance of control}} * 100$$

Antibacterial activity

The bacterial strains used for this study are *Escherichia coli* (MTCC 41), *Staphylococcus aureus* (MTCC 87), *Enterococcus faecalis* (ATCC 29212), *Streptococcus pyogenes* (ATCC 19615), *Pseudomonas aeruginosa (*clinical isolate), *Klebsiella pneumoniae* (MTCC 3384), *Chromobacterium violaceum* (ATCC 22019), *Proteus mirabilis* (clinical isolate) and *Listeria monocytogenes* (clinical isolate). Antimicrobial activity was checked using micro well dilution method. Gentamycin (1 mg/ml) was used as the positive control. Minimum inhibitory concentration (MIC) and Minimum bactericidal concentration (MBC) were calculated.

Antiproliferative activity

Cytotoxicity of the drug was tested against three cell lines – HCT116, K562 and HEK293. These cells were obtained from the National Centre for Cell Sciences (NCCS, Pune), and were maintained in DMEM and RPMI media supplemented with 10% FBS and antibiotics and was incubated at 37^0C in a humidified 5% CO_2 atmosphere. Toxicity of biogenic PINPs on normal cells was determined using freshly isolated human blood lymphocytes grown in RPMI media. MTT assay was performed according to Cheriyamundath et al. (2017) (Cheriyamundath et al. 2017). Cell viability was determined by calculating the difference between treated and untreated control groups and is given by:

$$\text{Percentage cell viability} = \frac{\text{Absorbance of control} - \text{absorbance of sample}}{\text{absorbance of control}} \times 100$$

Acridine orange—ethidium bromide dual staining

Dual staining was done to detect the evidence of apoptosis in biogenic PINPs treated cells. The control and treated cells were harvested by centrifugation at 800xg, washed with cold PBS (pH 7.4) and were adjusted to cell density of 1.5×10^5 cells /ml using PBS (pH 7.4). Acridine orange- ethidium bromide solution was taken in the ratio 1:1, was then added to the cell suspension at a final concentration of 100 µg/ml (Thangam et al. 2012) and was then observed under fluorescence microscope.

Larvicidal activity

Culex quinquefasciatus larvae were collected locally. The larvae were identified by Dr. Raghu, Centre for Disease Control, Kallayi, Kerala. Larvae were kept in plastic containers with tap water at room temperature under 13:10 h light and dark cycles (Chacko et al. 2015). PINPs were tested against first, second, third and fourth instar larvae. 20 larvae were released on each petri plate with 200 ml of water containing 1.0 ml of the desired concentration of the sample and mortality was observed after 24 h. The experiments were conducted under laboratory conditions at 25–30 ^{0} C. The percent mortality was recorded for an average of three replicates (Larvicides 2005; WHO, G. 1996; Patil et al. 2012). All experimental data was expressed as mean ± standard deviation.

$$\text{Percent mortality} = \frac{\%\ \text{test mortality} - \%\ \text{control mortality}}{100 - \%\ \text{control mortality}} \times 100$$

Dye degradation efficiency

Methylene Blue, an anionic dye, and Methyl Orange-a cationic dye was used for the study. To 8 ml of dyes (25 mg/l), 1 ml of H_2O_2 (10%), 1 ml of PINPs (10 mg/ml) or *P. korintii* aqueous extract (10 mg/ml) were added, the absorbance and color change was noted for 0–35 min at 5 min interval. The absorbance was recorded until the solution remained colorless. The absorbance of Methyl Orange was recorded at 460 nm and Methylene Blue at 660 nm. Analytical

determinations were made in triplicate (Badmapriya and Asharani 2016).

Result and discussions

Characterization of PINPs

In bio-green method, the formation of PINPs was indicated by a change in color of 0.01 M $FeCl_3$ from colorless to dark brown on addition *P. korintii* aqueous leaf extract in 2:3 ratio (Fig. 1). The color change in reaction mixture is due to excitation of surface plasmon vibration in the metal nanoparticles (Saranya et al. 2017). The UV–visible spectrum displayed a single and clear surface plasmon resonance band with wavelength around 350 nm (Fig. 2). Similar observations were reported by Pattanayak and Nayak (2013) (Pattanayak and Nayak 2013). The FTIR spectrum of PINPs displayed six sharp bands at 3370 cm^{-1}, 1629.07 cm^{-1}, 1402.96 cm^{-1}, 1027.39 cm^{-1}, 848.043 cm^{-1}, and 678.338 cm^{-1} (Fig. 3). The strong peak at 3370 cm^{-1} is due to strong alcoholic bonds like phenolics (Sathya et al. 2017; Hwang et al. 2014). 1629.07 cm^{-1} indicates the presence of C = C bonds that were accountable for the formation of PINPs (Mahdavi et al. 2013). Band 1402.96 cm^{-1} represents a C-H bond of methyl, methoxy, flavonoids and aromatic rings, 1027.39 cm^{-1} was attributed to the stretching vibration of C–O–C (Badni et al. 2016) and 848.043 cm^{-1} represents a C-O bond (Jędrzak et al. 2019). The strong peak at 678 cm^{-1} due to the inorganic stretching indicates the presence of INPs (Kanagasubbulakshmi and Kadirvelu 2017). The diffraction peaks at 2θ values of 16.7140, 26.550, 35.730, 55.600, 61.270 were found indexed to the (200), (201), (110), (312), (511) brag reflections. Multiple peaks obtained in the X- ray diffraction pattern thus confirm the crystalline nature of PINPs (Groiss et al. 2017). The diffraction peaks were evaluated using PANalytical Xpert Highscore software and they were found to be meghamite, Fe_2O_3(Fig. 4). From these evaluations, it was confirmed that the prepared biogenic nanoparticles are crystalline iron oxide (Fe_2O_3). The average size of PINPs was calculated using Scherrer"s formula and was found to be 49.86 nm. FESEM was employed to study the size, shape and morphology of the biosynthesized PINPs. The SEM images of the sample displayed in Fig. 5, reveal the predominantly spherical and relatively uniform shape of nanoparticles in the size range 40–60 nm. The average size of PINPs was determined from micrographic images and was found to be 48.53 ± 3.7 nm. The values were close to those determined by XRD analysis. The elemental composition of green synthesized iron nanoparticles was determined using EDX (Fig. 6). The peak of iron and oxygen were found and this further confirmed that the PINPs formed were iron oxide nanoparticles. C, O, P, Cl, Fe, S, K peaks were also observed approving the hypothesis that capping of the INPs was done using these compounds (Fig. 5).

(a) (b)

Fig. 1 Formation of PINPs: (**a**)The figure shows the colorless precursor solution (0.01 M $FeCl_3$), the solution immediately after mixing precursor and *P. korintii* leaves aqueous extract (2:3) and the solution obtained 12 h after continuous stirring at 60^0C. The color change of $FeCl_3$ solution from colorless to dark brown is the primary indication to the formation of iron nanoparticles (**b**). The PINPs

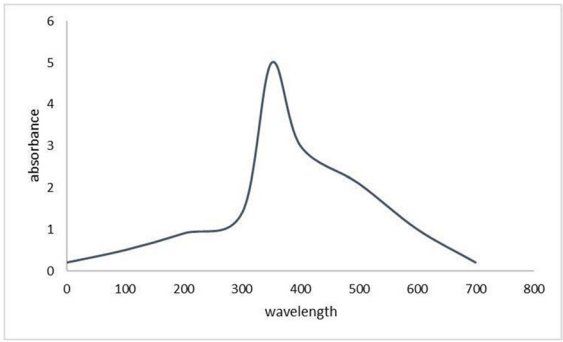

Fig. 2 UV–Vis absorption spectra of the green synthesized PINPs. A single and clear surface plasmon resonance band with wavelength around 350 nm is shown in the figure, which is in complete harmony with the UV spectral analysis of metallic iron

Phytochemical analysis

The *P. korintii* aqueous extract and PINPs were subjected to qualitative phytochemical analysis for the detection of phytoconstituents like alkaloids, flavonoids, terpenoids, phenolics, carbohydrates, saponins and proteins. The results are shown in Table 1. The results revealed the presence of alkaloids, flavonoids, terpenoids, phenolics, carbohydrates, saponins and protein compounds in the aqueous extract of *P. korintii,* while saponins and proteins were absent in PINPs. These may have been involved during the bioreduction process (i.e., conversion of ions to atoms) (Afreen et al. 2020).

Quantitative estimation of Total Phenolic Content (TPC)

A higher amount of phenolic content was observed in PINPs than *P. korintii* aqueous extract. The total phenolic content of synthesized PINPs was found to be 59.36 ± 1.64 µg GAE/mg as compared to *P. korintii* aqueous extract phenolic content (17.2 ± 0.1 µg GAE/mg). Similar observations have been reported by Afreen et al. (2020) and Zahra et al. (2017) (Afreen et al. 2020; Zahra et al. 2017).

In vitro antioxidant assays

The DPPH free radical scavenging antioxidant activity of PINPs and *P. korintii* aqueous extract was assessed and compared with ascorbic acid (Fig. 7). The extract and PINPs exhibited dose-dependent scavenging activity. At the highest concentration tested, PINPs exhibited higher DPPH scavenging activity, 89.78 ± 0.07% than *P. korintii* aqueous extract, 72.45 ± 0.89%. ABTS cation radical scavenging activity was 28.7 ± 0.21%—58.7 ± 0.12% at a concentration range of 100–1000 µg/ml for the PINP and 0.98 ± 1.23%—25 ± 0.56% activity for *P. korintii* aqueous extract (Fig. 8). The higher tendency to interact and reduce DPPH free electrons by PINPs than *P. korintii* aqueous extract could be attributed to the high surface area to volume ratio and higher polyphenol content.

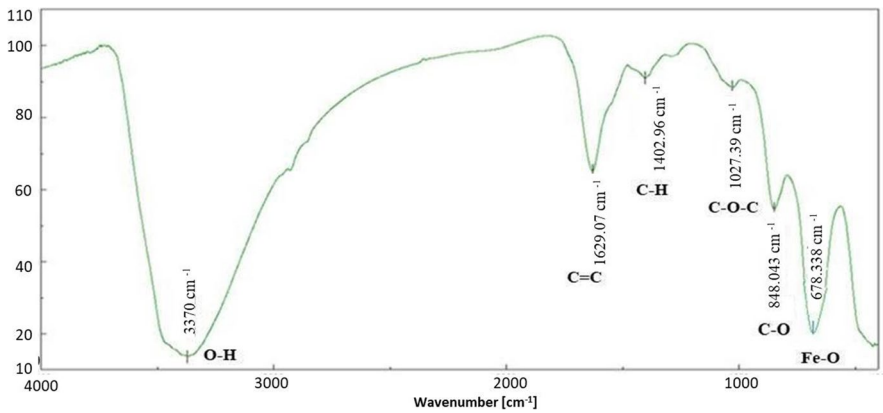

Fig. 3 FTIR spectra of PINPs. The figure shows the infrared spectrum of *P. korintii* phytoconstituents involved in the capping and bio reducing of the biogenic PINPs

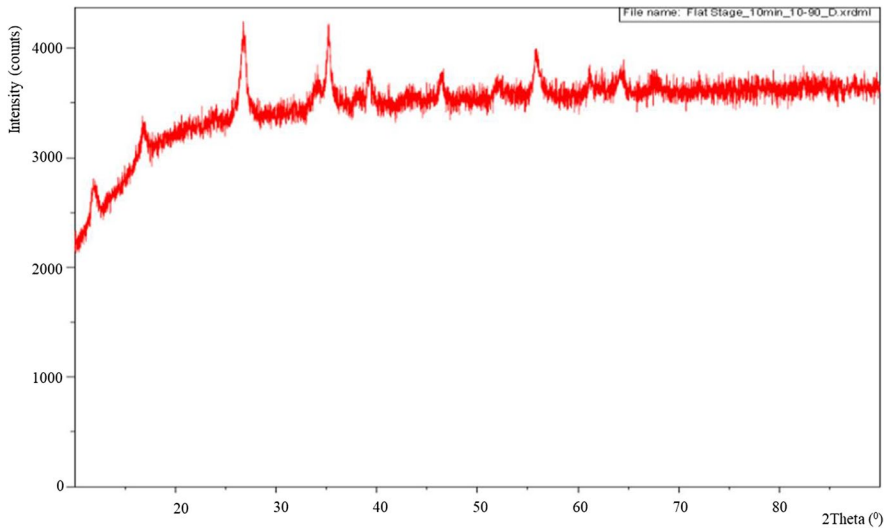

Fig. 4 X- ray diffraction pattern of PINPs. The nature and phase composition of INPs were determined by XRD analysis with Braggs angle ranging from 10^0—70^0. Defined peaks around 28^0—29^0 describing Meghamite (Υ-Fe_2O_3) and other dominant peaks due to the presence of extract phytochemicals were observed. The diffraction peaks at 2θ values of 16.7140, 26.550 (201), 35.730, 55.600 (312), 61.270 (511) evaluated using PANalytical Xpert Highscore software confirming the crystalline iron oxide nature of PINPs

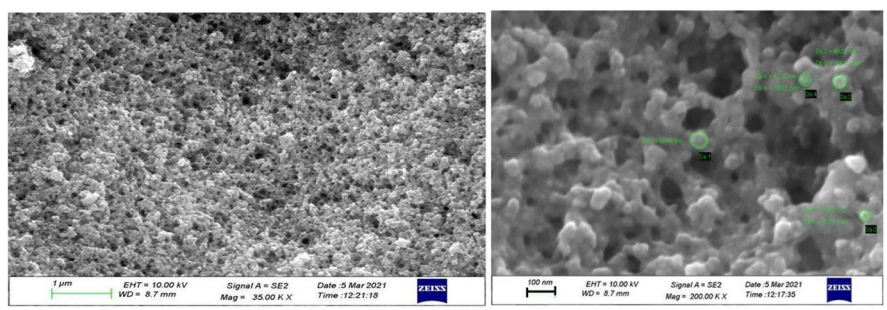

(a) (b)

Fig. 5 SEM image of PINPs. The figures show (**a**) low and (**b**) high magnification images of green synthesised PINPs that are spherical in nature with diameters ranging from 40–60 nm

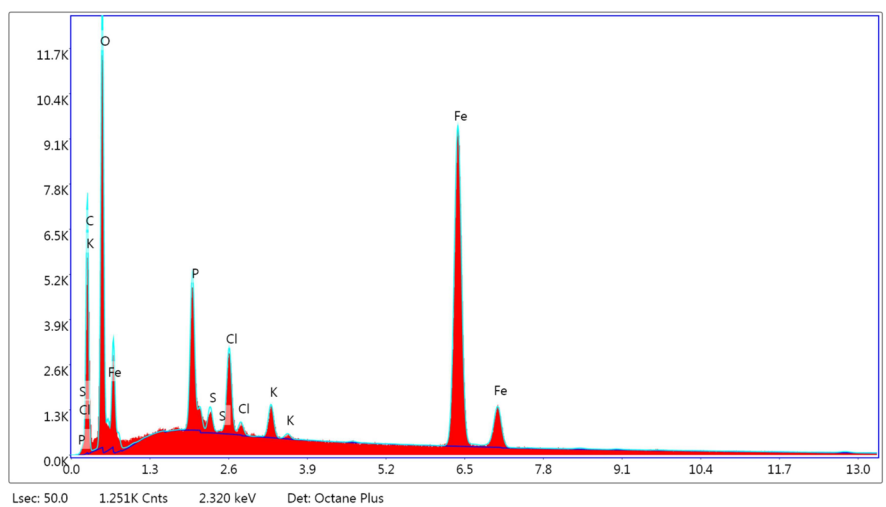

Fig. 6 Energy Dispersive X-ray Spectroscopy (EDX) image representing the elemental composition in PINPs

Table 1 Qualitative phytochemical analysis of plant extracts v/s PINPs

Sl. No	Phytochemicals	*P. korintii* aqueous extract	PINPs
1	Alkaloids	Positive	Positive
2	Flavonoids	Positive	Positive
3	Terpenoids	Positive	Positive
4	Phenolics	Positive	Positive
5	Carbohydrate	Positive	Positive
6	Saponins	Positive	Negative
7	Proteins	Positive	Negative

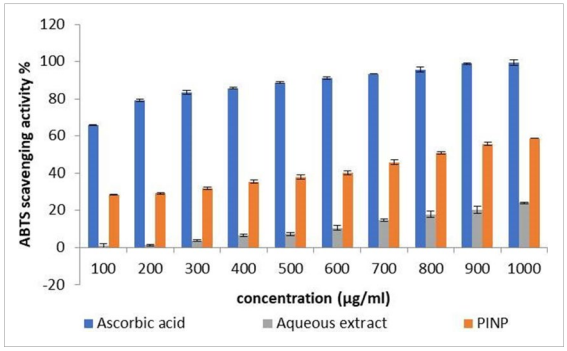

Fig. 8 ABTS Radical Scavenging activity of PINP, precursor aqueous extract and the standard, ascorbic acid (values represent mean ± S.D. of three experiments)

Antibacterial activity

The antibacterial activity was evaluated against diffrent gram positive bacteria– *S. aureus, L. monocytogenes, E. faecalis, S. pyogenes* and gram negative bacteria—*E. coli*, *P. aeruginosa, K. pneumonia, C. violaceum,* and *P. mirabilis* by microwell dilution method. PINPs exhibited significant antibacterial activity compared to *P. korintii* aqueous extract. Even at the highest concentration tested, the aqueous extract was unable to produce greater than a 50% detrimental effect on the initial load of bacteria, while the last dilution of PINPs was sufficient enough to kill 50% of the starting inoculum. PINPs were more effective against *Enterococcus faecalis* and *Klebsiella pneumoniae.* Figure 9 (a) shows the susceptibility of tested organisms to aqueous extract and Fig. 9 (b) exhibits the potent antibacterial activity of PINPs. MIC and MBC values were calculated and depicted in Table 2.

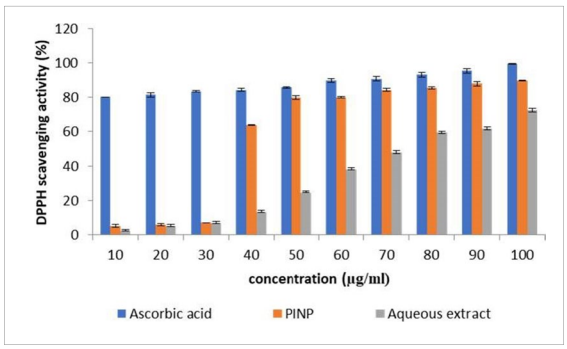

Fig. 7 DPPH Free Radical Scavenging activity of PINP, aqueous extract and the standard, ascorbic acid (values represent mean ± S.D. of three experiments)

Antiproliferative activity of PINPs

Cancer cells treated with varying concentrations of PINPs and *P. korintii* aqueous extract for 24, 48 and 72 h were subjected to MTT assay. The *P. korintii* aqueous extract showed considerably less antiproliferative potential, i.e., viability of cells > 80% even at the highest concentration tested (100 ug/ml) on HCT 116 and K562 cell lines. The PINPs exhibited remarkable anti-proliferative activity on the cell lines tested, which became visible at 48 h (Table 3). Freshly isolated human lymphocytes and HEK cell line were also used to evaluate the cytotoxicity activity. The results clearly indicated that none of the samples displayed any toxicity towards the human lymphocytes. At the IC_{50} concentrations exhibited by PINPs (85 ug/ml), the viability of lymphocytes was more than 80%.

The extent of hemolysis was studied in human erythrocytes at concentrations ranging from 50–200 ug/ml. The PINPs and the extract failed to show any

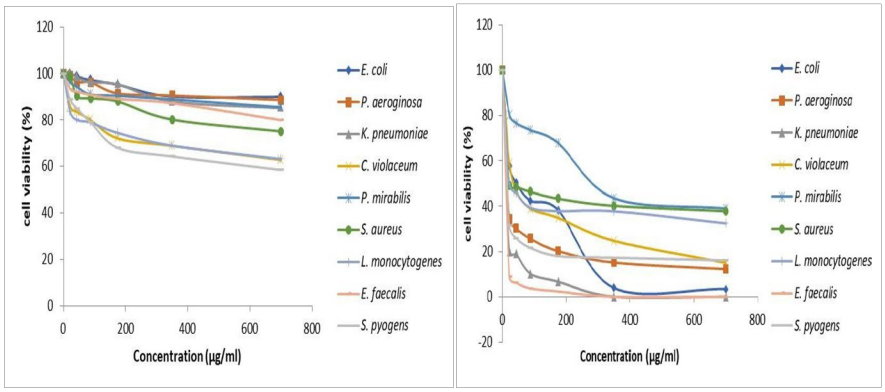

Fig. 9 Antibacterial activity determined using micro well dilution method (**a**)*P. korintii* aqueous extract (**b**) PINPs

Table 2 Antibacterial activity (MBC and MIC) of *P. korintii* leaves aqueous extract and PINPs against human pathogens

Organism	PINP		*P. korintii* aqueous extract	
	MIC (µg/ml)	MBC (µg/ml)	MIC (µg/ml)	MBC (µg/ml)
Staphylococcus aureus	21.875 ± 1.4	87.5	2200 ± 1.1	4000
Listeria monocytogenes	21.875 ± 1.7	87.5	2500 ± 1.5	5000
Enterococcus faecalis	10.53 ± 1.3	43.75	2200 ± 1.5	4000
Streptococcus pyogenes	15.32 ± 0.8	87.5	3000 ± 1.6	5000
Escherichia coli	43.75 ± 2.8	175	1900 ± 1.9	3000
Pseudomonas aeruginosa	15.875 ± 2.7	87.5	2800 ± 2.3	5000
Klebsiella pneumoniae	10.937 ± 2.7	43.75	2200 ± 2.7	4000
Chromobacterium violaceum	40.75 ± 2.1	175	2500 ± 3	5000
Proteus mirabilis	350 ± 0.8	700	2100 ± 0.9	3000

toxicity towards them (hemolysis is less than 10%). Triton X-100 was used as positive control. Figure 10 shows the extent of hemolysis exerted by PINPs and aqueous extract.

Cytomorphological studies showed dose-dependent cytotoxicity of biogenic PINPs and a considerable reduction in cell number was observed as a result of a decrease in cell proliferation. This may be due to their cytotoxic mode of action rather than just inhibiting growth or blocking cell cycle progression. 'Blebbing' on the surface of the membrane and loss of membrane integrity, typical characteristics apparent in apoptotic cells were also visualized (Fig. 11). These morphological changes observed with treatment are indicative of the induction of apoptosis.

Table 3 Antiproliferative effects (IC_{50} values using MTT assay) of *P. korintii* leaves aqueous extract and PINP on different cell lines and lymphocytes

Cells	*P. korintii* aqueous extract IC_{50} values (ug/ml)			PINPs IC_{50} values (ug/ml)		
	24 h	48 h	72 h	24 h	48 h	72 h
K562	> 100	> 100	> 100	> 100	84.99 ± 4.3	72.32 ± 2.4
HCT116	> 100	> 100	> 100	> 100	79.70 ± 6.2	75.26 ± 2.5
HEK	> 200	> 200	> 200	> 200	> 200	> 200
Lymphocytes	> 200	> 200	> 200	> 200	> 200	> 200

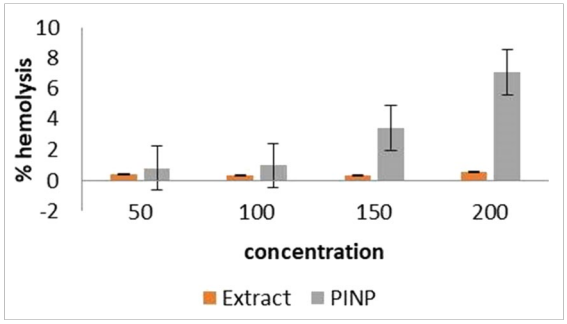

Fig. 10 Cytotoxicity evaluation of biogenic PINPs against human erythrocytes. Toxicity was measured as percentage haemolysis. Values represent the mean ± S.D. of three experiments

Acridine-orange ethidium bromide dual staining

In the dual staining technique, normal cells are characterized by possession of uniformly bright green intact chromatin nuclei; early to late apoptotic cells contain condensed or fragmented chromatin with yellow green and orange nuclei, and necrotic cells have nuclei stained orange. In the study, HCT 116 and K562 cells treated with PINPs showed late apoptotic cells (Fig. 12). The data thus confirms the induction of apoptosis by PINPs in K562 and HCT116 cells.

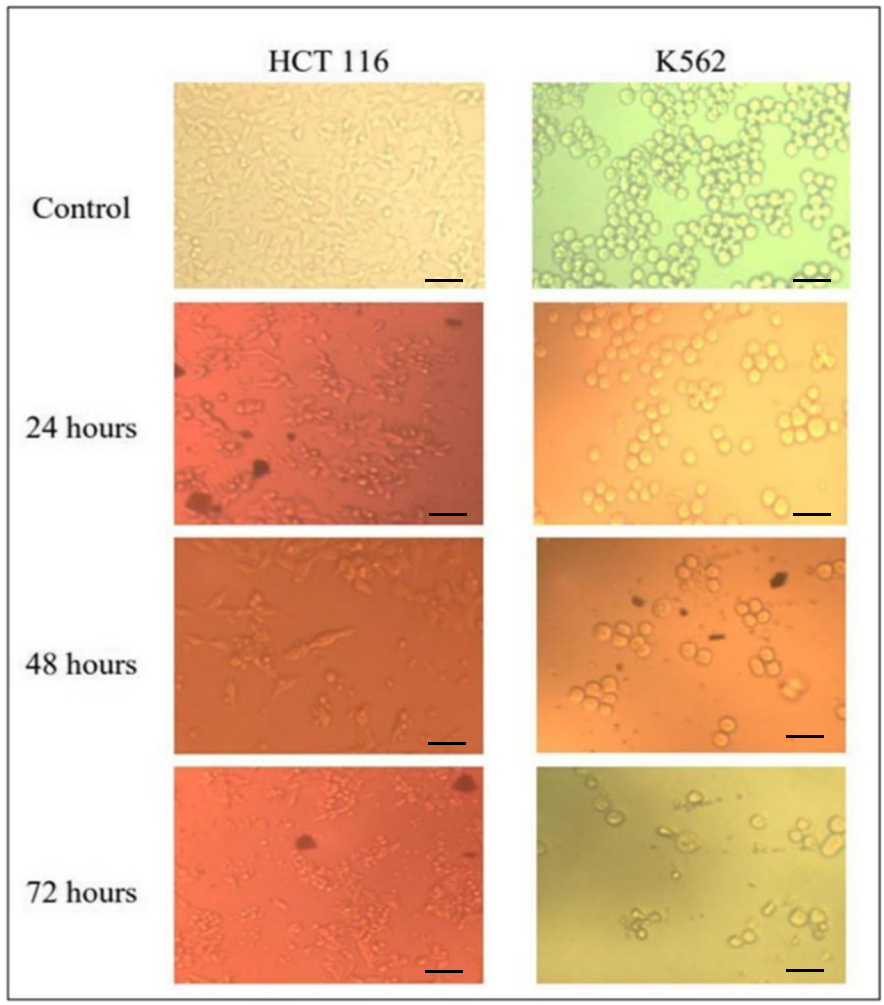

Fig. 11 Morphological changes of the cells on treatment with PINP. *Scale bar represents 30 µm*

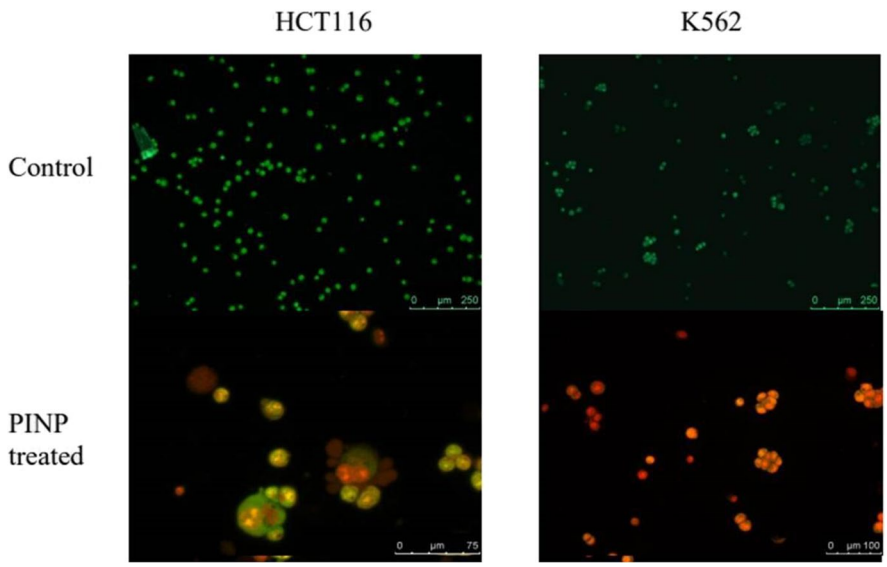

Fig. 12 Apoptosis induction in HCT 116 and K562 cells treated with PINPs stained with AO/EtBr

Larvicidal activity

Culex quinquefasciatus, the common southern house mosquito is the vector of pathogens like *Wuchereria bancrofti*, Avian malaria, arboviruses, etc. PINPs gave promising activity against larvae of *C. quinquefasciatus* (Table 4). The hypothesized mechanism behind larvicidal activity is due to the binding of iron nanoparticles to the enzyme systems of larvae and cell membrane disruption and this ease in access of nanoparticles is due to their increased surface area to volume ratio, thus thereby increasing their action against larva (Sutthanont et al. 2019). These results suggest that the PINPs can be employed to develop effective biocides for controlling the target vector mosquitoes.

LC50: concentration at which PINPs kill 50% of exposed larvae.

Table 4 Toxicity (LC 50) of PINPs against larvae of *Culex quinquefasciatus*

Mosquito larvae	LC50 value (in mg/L)
First instar larvae	40 ± 1.5
Second instar larvae	45 ± 0.8
Third instar larvae	99 ± 2.1
Fourth instar larvae	120 ± 3.5

Dye degradation activity

One of the efficient applications of INPs is dye degradation, so PINPs were analyzed for its environmental application in degradation of textile dyes commonly found in industrial wastes. Methyl orange is an anionic azo dye which is soluble in water, stable, non-biodegradable and hard to remove by conventional treatments. They are toxic, may cause diarrhea and nausea, and at high concentrations can be fatal (Amenaghawon et al. 2022; Carolin et al. 2021; Wu et al. 2021; Raliya et al. 2017; Zyoud and Zu'bi, A., Helal, M.H., Park, D., Campet, G. and Hilal, H.S. 2015). Methylene blue, a phenothiazine derivative, is yet another toxic and carcinogenic dye which is hard to remove from textile effluents (Appavu et al. 2018). Fenton reaction utilizes ions to react with hydrogen peroxide, producing hydroxyl radicals with powerful oxidizing ability to degrade organic pollutants.

Catalytic degradation of methyl orange and methylene blue was carried out using green synthesized PINPs in the presence of 10% H_2O_2 and was initially recognized by change in color. The residual concentration of dye was measured from absorbance at 460 nm for Methyl Orange and 660 nm for Methylene Blue. The absorption spectrum of the dyes decreased gradually over a time range of 35 min, which indicates the catalytic degradation of the dyes. Without the metal catalyst, the mixture of H_2O_2 and the dyes did not show any degradation. The reaction was followed until

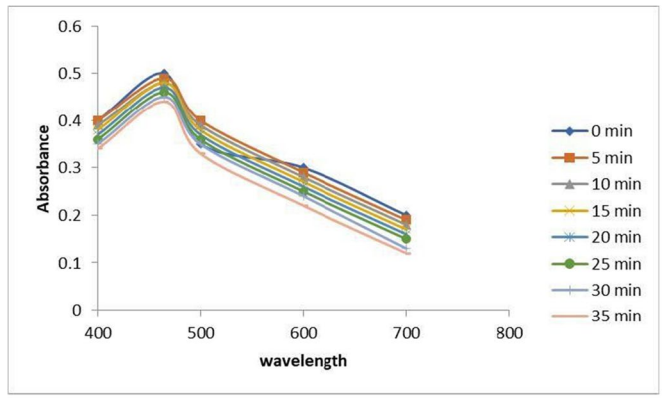

(a)

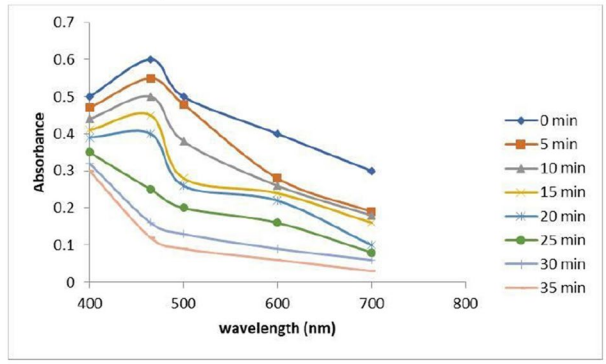

(b)

(c)

Fig. 13 Time-dependent UV–Vis absorption spectra of Methyl orange in the presence of (**a**) aqueous extract and H_2O_2 (**b**) PINP and H_2O_2. (**c**)Change in color of methyl orange before and after treatment with PINPs

the absorbance of dyes approached the baseline and the dyes were colorless (Fig. 13a). However, *P. korintii* aqueous extract was ineffective in catalyzing the degradation of dyes (Fig. 14b.). The results suggest that the reduction of dyes with INPs occurs at a fast rate in a few minutes. These indicate that by employing PINPs as catalyst and hydrogen peroxide as an oxidant, methyl orange and methylene blue can be effectively degraded in a fenton-like reaction mechanism. Figure 13c shows the color change exhibited before degradation and after treatment with PINPs.

Conclusion

An ecofriendly, cost-effective and cleaner biosynthesis process has been successfully employed for the synthesis of iron oxide nanoparticles using leaf extract of *P. korintii*. Phytochemical analysis showed the presence of diverse classes of secondary metabolites like alkaloids, flavonoids, terpenoids, phenolics and carbohydrates in PINPs and alkaloids, flavonoids, terpenoids, phenolics, carbohydrates, saponins and proteins in *P. korintii* aqueous extract. As evident by the ability to scavenge DPPH free radicals and ABTS cations, these activities points to their potential application in the development of antioxidant-based products and therapies. PINPs demonstrated antibacterial efficacy against both gram-positive and gram-negative bacteria, suggesting that they might be used as an antimicrobial agent. In K562 and HCT116 cells, the PINPs effectively induced apoptosis leading to cell death. Importantly, the nanoparticles showed selective toxicity, meaning they had minimal harmful effects on lymphocytes, HEK293 cells, and erythrocytes. This raises the probability of employing them as anti-cancer agents potential for targeted therapies with reduced side effects. The toxicity assessment of the nanoparticles against *Culex quinquefasciatus* larvae showed

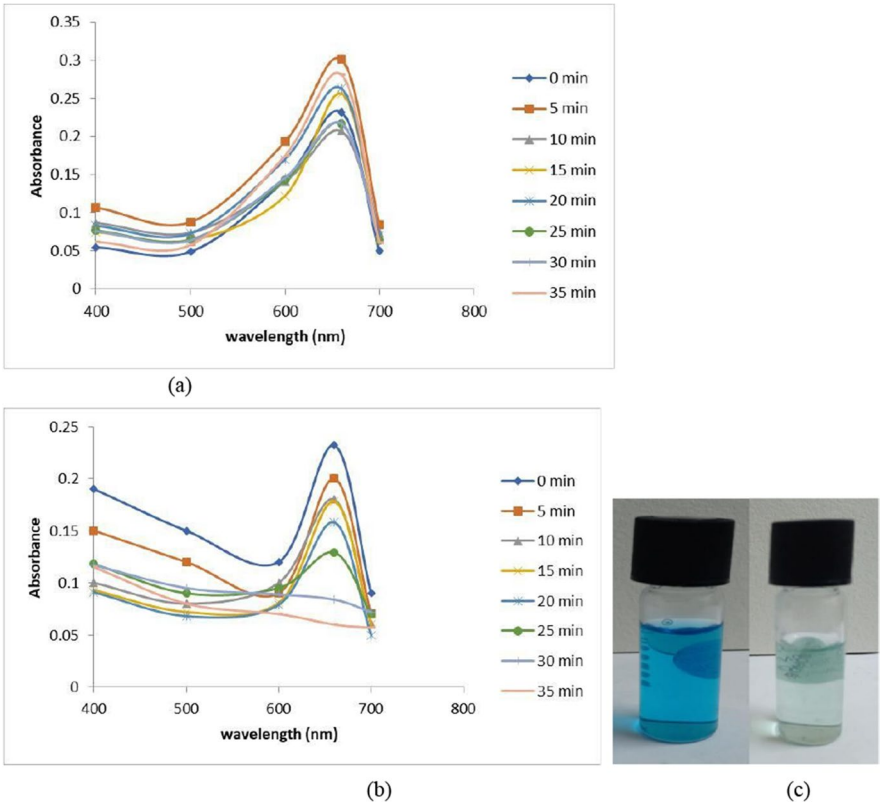

Fig. 14 Time-dependent UV–Vis absorption spectra of Methylene blue in the presence of (**a**) aqueous extract and H_2O_2 (**b**) PINP and H_2O_2. (**c**)Change in color of dye before and after treatment with PINP

promising results, indicating their possible use as an effective insecticide against mosquito larvae. The nanoparticles also exhibited catalytic activity in the degradation of textile dyes, such as methylene blue and methyl orange, through a Fenton-like reaction. This suggests their prospective application in wastewater treatment or bioremediation. Overall, the findings of this study have significant implications for the practical applications of these iron oxide nanoparticles in various fields, including medicine, insect control, and bioremediation.

Acknowledgements The authors acknowledge University of Calicut for fellowship awarded to Hana Mol K.E. during M.Phil degree. The authors also acknowledge UGC and Ministry of Minority Affairs, Government of India for the research fellowship awarded to Tancia Rosalin. The CSIF, University of Calicut is acknowledged for providing sophisticated experimental facilities. Acknowledgement is also due to University of Calicut and Department of Biotechnology, New Delhi for providing the infrastructural facilities to carry out the research.

Authors' contribution HKE: Conceptualization, Investigation, Methodology, Writing – original draft. TR: Investigation, Interpretation of data, Writing – original draft, Drafting the manuscript. KKE: Conceptualization, Writing – original draft, Writing – review & editing.

Funding This research did not receive any specific grant from funding agencies in the public, commercial, or not-for-profit sectors.

Declarations

Competing interest The authors declare no competing interests.

References

Afreen A, Ahmed R, Mehboob S, Tariq M, Alghamdi HA, Zahid AA, Ali I, Malik K, Hasan A (2020) Phytochemical-assisted biosynthesis of silver nanoparticles from *Ajuga bracteosa* for biomedical applications. Materials Research Express 7(7):075404 (https://iopscience.iop.org/article/10.1088/2053-1591/aba5d0)

Ali A, Shah T, Ullah R, Zhou P, Guo M, Ovais M, Tan Z, Rui Y (2021) Review on recent progress in magnetic nanoparticles: Synthesis, characterization, and diverse applications. Front Chem 9:629054. https://doi.org/10.3389/fchem.2021.629054

Amenaghawon AN, Anyalewechi CL, Darmokoesoemo H, Kusuma HS (2022) Hydroxyapatite-based adsorbents:

Applications in sequestering heavy metals and dyes. J Environ Manage 302:113989. https://doi.org/10.1016/j.jenvman.2021.113989

Anik MI, Hossain MK, Hossain I, Mahfuz AMUB, Rahman MT, Ahmed I (2021) Recent progress of magnetic nanoparticles in biomedical applications: A review. Nano Select 2(6):1146–1186. https://doi.org/10.1002/nano.202000162

Appavu B, Thiripuranthagan S, Ranganathan S, Erusappan E, Kannan K (2018) BiVO4/N-rGO nano composites as highly efficient visible active photocatalyst for the degradation of dyes and antibiotics in eco system. Ecotoxicol Environ Saf 151:118–126. https://doi.org/10.1016/j.ecoenv.2018.01.008

Ashton MS, Gunatilleke S, De Zoysa N, Dassanayake MD, Gunatilleke N, Wijesundera S (1997) A field guide to the common trees and shrubs of Sri Lanka, WHT Publications (Pvt.) Ltd., Sri Lanka. p. 432

Avasthi A, Caro C, Pozo-Torres E, Leal MP, García-Martín ML (2020) Magnetic nanoparticles as MRI contrast agents. Surface-modified Nanobiomaterials for Electrochemical and Biomedicine Applications, pp.49–91. https://doi.org/10.1007/s41061-021-00340-y

Badmapriya D, Asharani IV (2016) Dye degradation studies catalysed by green synthesized iron oxide nanoparticles. Int J ChemTech Res 9(6):409–416

Badni, N., Benheraoua, F.Z., Tadjer, B., Boudjemaa, A., El Hameur, H. and Bachari, K. (2016). Green synthesis of α-Fe2O3 nanoparticles using Roman nettle. http://depot.umc.edu.dz/handle/123456789/12347

Basha S, Rajyalakshmi E, Maheswari P, Rambabu M (2014) Tribal medicinal plants of Kambakam Hills, Eastern Ghats, Andhra Pradesh, India. J Econ Taxon Botany 38(1)

Beheshtkhoo N, Kouhbanani MAJ, Savardashtaki A, Amani AM, Taghizadeh S (2018) Green synthesis of iron oxide nanoparticles by aqueous leaf extract of *Daphne mezereum* as a novel dye removing material. Appl Phys A 124:1–7. https://doi.org/10.1007/s00339-018-1782-3

Bhakya S, Muthukrishnan S, Sukumaran M, Muthukumar M (2016) Biogenic synthesis of silver nanoparticles and their antioxidant and antibacterial activity. Appl Nanosci 6:755–766. https://doi.org/10.1007/s13204-015-0473-z

Bijauliya RK, Jain SK, Alok S, Dixit V, Singh VK (2017) Macroscopical, microscopical and physico-chemical studies on leaves of *Dalbergia sissoo* Linn (Fabaceae). Int J Pharm Sci Res 8(4):1864. https://ijpsr.com/bf t-article/macroscopical-microscopical-and-physico-chemical-studies-on-leaves-of-dalbergia-sissoo-linn fabaceae/?view=fulltext

Cai X, Gao Y, Sun Q, Chen Z, Megharaj M, Naidu R (2014) Removal of co-contaminants Cu (II) and nitrate from aqueous solution using kaolin-Fe/Ni nanoparticles. Chem Eng J 244:19–26. https://doi.org/10.1016/j.cej.2014.01.040

Carolin CF, Kumar PS, Joshiba GJ (2021) Sustainable approach to decolourize methyl orange dye from aqueous solution using novel bacterial strain and its metabolites characterization. Clean Technol Environ Policy 23:173–181. https://doi.org/10.1007/s10098-020-01934-8

Chacko A, Christy PH, Kavya KS (2015) Study on larvicidal activity of crude extracts of *Ruta graveolens* against Aedes aegypti and Anopheles stephensi. International Journal of Mosquito Research 2(4):01–06 (https://www.dipterajournal.com/vol2issue4/pdf/2-2-59.1.pdf)

Chan MH, Li CH, Chang YC, Hsiao M (2022) Iron-Based Ceramic Composite Nanomaterials for Magnetic Fluid Hyperthermia and Drug Delivery. Pharmaceutics 14(12):2584. https://doi.org/10.3390/pharmaceutics14122584

Cheriyamundath S, Raghavan R, Banerji A, Klika KD, Ulrich C, Owen RW, Madassery J (2017) Bioassay-guided isolation and evaluation of antiproliferative effects of (Z)-ethylidene-4, 6-dimethoxycoumaran-3-one from Pogostemon Quadrifolius (Benth). Asian Pacific J Cancer Prevent 18(7):1783. https://doi.org/10.22034/APJCP.2017.18.7.1783

Da Rosa Salles T, Da Silva Bruckamann F, Viana AR, Krause LMF, Mortari SR, Rhoden CRB (2022) Magnetic nanocrystalline cellulose: Azithromycin adsorption and in vitro biological activity against melanoma cells. J Polym Environ 30(7):2695–2713. https://doi.org/10.1007/s10924-022-02388-3

Devatha CP, Thalla AK, Katte SY (2016) Green synthesis of iron nanoparticles using different leaf extracts for treatment of domestic waste water. J Clean Prod 139:1425–1435. https://doi.org/10.1016/j.jclepro.2016.09.019

Groiss S, Selvaraj R, Varadavenkatesan T, Vinayagam R (2017) Structural characterization, antibacterial and catalytic effect of iron oxide nanoparticles synthesised using the leaf extract of *Cynometra ramiflora*. J Mol Struct 1128:572–578. https://doi.org/10.1016/j.molstruc.2016.09.031

Gupta S, Prakash J (2009) Studies on Indian green leafy vegetables for their antioxidant activity. Plant Foods Hum Nutr 64:39–45. https://doi.org/10.1007/s11130-008-0096-6

Hassan H, Hameed BH (2011) Fe–clay as effective heterogeneous Fenton catalyst for the decolorization of Reactive Blue 4. Chem Eng J 171(3):912–918. https://doi.org/10.1016/j.cej.2011.04.040

Hwang SW, Umar A, Dar GN, Kim SH, Badran RI (2014) Synthesis and characterization of iron oxide nanoparticles for phenyl hydrazine sensor applications. Sens Lett 12(1):97–101. https://doi.org/10.1166/sl.2014.3224

Jędrzak A, Rębiś T, Kuznowicz M, Jesionowski T (2019) Bioinspired magnetite/lignin/polydopamine-glucose oxidase biosensing nanoplatform. From synthesis, via sensing assays to comparison with others glucose testing techniques. Int J Biol Macromol 127:677–682. https://doi.org/10.1016/j.ijbiomac.2019.02.008

Kanagasubbulakshmi, S. and Kadirvelu, K. (2017). Green synthesis of iron oxide nanoparticles using *Lagenaria siceraria* and evaluation of its antimicrobial activity. Defence Life Science Journal, 2(4), pp.422–427. https://doi.org/10.14429/dlsj.2.12277

Larvicides M.O.S.Q.U.I.T.O (2005) Guidelines for laboratory and field testing of mosquito larvicides. http://apps.who.int/iris/bitstream/handle/10665/69101/WHO_CDS_WHOPES_GCDPP_2005.13.pdf?sequence=1

Mahdavi M, Namvar F, Ahmad MB, Mohamad R (2013) Green biosynthesis and characterization of magnetic iron oxide (Fe3O4) nanoparticles using seaweed (*Sargassum muticum*) aqueous extract. Molecules 18(5):5954–5964. https://doi.org/10.3390/molecules18055954

Makarov VV, Love AJ, Sinitsyna OV, Makarova SS, Yaminsky IV, Taliansky ME, Kalinina NO (2014) "Green" nanotechnologies: synthesis of metal nanoparticles using plants. Acta Naturae 6(1):35–44

Nunes FB, da Silva Bruckmann F, da Rosa Salles T, Rhoden CRB (2023) Study of phenobarbital removal from the

aqueous solutions employing magnetite-functionalized chitosan. Environ Sci Pollut Res 30(5):12658–12671. https://doi.org/10.1007/s11356-022-23075-9

Patil CD, Patil SV, Borase HP, Salunke BK, Salunkhe RB (2012) Larvicidal activity of silver nanoparticles synthesized using *Plumeria rubra* plant latex against Aedes aegypti and Anopheles stephensi. Parasitol Res 110:1815–1822. https://doi.org/10.1007/s00436-011-2704-x

Pattanayak M, Nayak PL (2013) Ecofriendly green synthesis of iron nanoparticles from various plants and spices extract. Int J Plant, Animal Environ Sci 3(1):68–78

Poguberović SS, Krčmar DM, Maletić SP, Kónya Z, Pilipović DDT, Kerkez DV, Rončević SD (2016) Removal of As (III) and Cr (VI) from aqueous solutions using "green" zero-valent iron nanoparticles produced by oak, mulberry and cherry leaf extracts. Ecol Eng 90:42–49. https://doi.org/10.1016/j.ecoleng.2016.01.083

Poovathur P, Joseph S (2016) An Ethnopharmacological survey on medicinal plants from sacred grove of Sree Puthiya Bhagavathi Temple, Kalloori, Kannur (Dist), Kerala. Int J Adv Sci Res 1(8):24–35

Raliya R, Avery C, Chakrabarti S, Biswas P (2017) Photocatalytic degradation of methyl orange dye by pristine titanium dioxide, zinc oxide, and graphene oxide nanostructures and their composites under visible light irradiation. Appl Nanosci 7:253–259. https://doi.org/10.1007/s13204-017-0565-z

Rashmi V, Prabhushankar HB, Sanjay KR (2021) Centella asiatica L. callus mediated biosynthesis of silver nanoparticles, optimization using central composite design, and study on their antioxidant activity. Plant Cell Tissue Organ Culture (PCTOC) 146(3):515–529. https://doi.org/10.1007/s11240-021-02086-3

Richard PSS, Muthukumar SA (2012) Arborescent angiosperms of Mundanthurai range in the Kalakad-Mundanthurai Tiger Reserve (KMTR) of the southern Western Ghats India. Check List 8(5):951–962. https://doi.org/10.15560/8.5.951

Rosalin T, Elyas KK (2018) Pharmacognostical and physicochemical evaluation of an indo-sri lankan ethnomedicinal plant species Polyalthia korinti (Dunal) Benth. & Hook F. Int J Pharmaceutical Sci Res 9(10):4355–4360

Saranya S, Vijayarani K, Pavithra S (2017) Green Synthesis of Iron Nanoparticles using Aqueous Extract of *Musa ornata* Flower Sheath against Pathogenic Bacteria. Indian J Pharm Sci 79(5):688–694

Sathya K, Saravanathamizhan R, Baskar G (2017) Ultrasound assisted phytosynthesis of iron oxide nanoparticle. Ultrason Sonochem 39:446–451. https://doi.org/10.1016/j.ultsonch.2017.05.017

Sekhar J, Sudarsanam GPPG, Prasad GP (2011) Ethnic information on treatments for snake bites in kadapa district of Andhra Pradesh. Life Sciences Leaflets 12:368–375

Sharma JK, Easa PS, Mathew G (2003) Monitoring biodiversity in selected landscapes in the Kerala part of Western Ghats. KFRI research report no. 283. ed.: Kerala Forest Research Institute. Peechi, Thrissur, India, 182 pp

Silva AC, Oliveira TR, Mamani JB, Malheiros SM, Malavolta L, Pavon LF, Sibov TT, Amaro Jr E, Tannús A, Vidoto EL, Martins MJ (2011) Application of hyperthermia induced by superparamagnetic iron oxide nanoparticles in glioma treatment. Int J Nanomed 591–603. https://doi.org/10.2147/IJN.S14737

Sutthanont N, Attrapadung S, Nuchprayoon S (2019) Larvicidal activity of synthesized silver nanoparticles from *Curcuma zedoaria* essential oil against Culex quinquefasciatus. Insects 10(1):27. https://doi.org/10.3390/insects10010027

Swathi BR, Joseph S (2017) Floristic composition and ethnomedicinal practices of iriveri sree Pulideva temple, Kannur district. Kerala Int J Botany Stud 2(3):16–24

Tahir K, Nazir S, Ahmad A, Li B, Shah SAA, Khan AU, Khan GM, Khan QU, Khan ZUH, Khan FU (2016) Biodirected synthesis of palladium nanoparticles using *Phoenix dactylifera* leaves extract and their size dependent biomedical and catalytic applications. RSC Adv 6(89):85903–85916. https://doi.org/10.1039/C6RA11409A

Thangam R, Gunasekaran P, Kaveri K, Sridevi G, Sundarraj S, Paulpandi M, Kannan S (2012) A novel disintegrin protein from *Naja naja* venom induces cytotoxicity and apoptosis in human cancer cell lines in vitro. Process Biochem 47(8):1243–1249. https://doi.org/10.1016/j.procbio.2012.04.020

Turakhia B, Turakhia P, Shah S (2018) Green synthesis of zero valent iron nanoparticles from *Spinacia oleracea* (spinach) and its application in waste water treatment. J Adv Res Appl Sci 5(1):46–51

Vivek R, Thangam R, Muthuchelian K, Gunasekaran P, Kaveri K, Kannan S (2012) Green biosynthesis of silver nanoparticles from *Annona squamosa* leaf extract and its in vitro cytotoxic effect on MCF-7 cells. Process Biochem 47(12):2405–2410. https://doi.org/10.1016/j.procbio.2012.09.025

WHO G (1996) Report of the WHO Informal Consultation on the Evaluation and Testing of Insecticides. World Health Organization Geneva 10:1026–1032

Wu L, Liu X, Lv G, Zhu R, Tian L, Liu M, Li Y, Rao W, Liu T, Liao L (2021) Study on the adsorption properties of methyl orange by natural one-dimensional nano-mineral materials with different structures. Sci Rep 11(1):10640. https://doi.org/10.1038/s41598-021-90235-1

Yalcin S, Gündüz U (2021) Iron oxide-based polymeric magnetic nanoparticles for drug and gene delivery: in vitro and in vivo applications in cancer. Handbook of polymer and ceramic nanotechnology, pp.1271–1292. https://doi.org/10.1007/978-3-030-40513-7_38

Zahra SS, Ahmed M, Qasim M, Gul B, Zia M, Mirza B, Haq IU (2017) Polarity based characterization of biologically active extracts of Ajuga bracteosa Wall. ex Benth. and RP-HPLC analysis. BMC Complement Alternative Med 17(1):1–16

Zyoud A, Zu'bi A, Helal MH, Park D, Campet G, Hilal HS (2015) Optimizing photo-mineralization of aqueous methyl orange by nano-ZnO catalyst under simulated natural conditions. J Environ Health Sci Eng 13:1-10https://doi.org/10.1186/s40201-015-0204-0